Freezing the orientation of a nematic stretched elastomer by photocrosslinking

Giulio Malucelli [a], Pio Iannelli [b], Marta Giamberini [c,*]

[a] Politecnico di Torino, Dipartimento di Scienza dei Materiali ed Ingegneria Chimica, C.so Duca degli Abruzzi 24, 10129 Torino, Italy
[b] Università di Salerno, Dipartimento di Scienze Farmaceutiche, Via Ponte don Melillo, 84084 Fisciano, Salerno, Italy
[c] Universitat Rovira i Virgili, Departament d'Enginyeria Química, Av. Països Catalans, 26, 43007 Tarragona, Spain

ARTICLE INFO

ABSTRACT

In this paper we tried to prepare shape memory main chain LC materials, by photopolymerizing (UV-curing) LC elastomers subjected to uniaxial stress. For this purpose, we prepared blends, having different compositions, of a well-known mesogenic diglycidyl-terminated monomer, namely 4,4′-diglycidyloxy-biphenyl (DIF), with its homologous bearing lateral photocurable allyl groups (AllDIF). The obtained blends were thermally cured with an aliphatic diacid (decandioic acid, SA), and gave LC networks in all the cases but 100% AllDIF composition. LC networks corresponding to a selected blend composition were subsequently conditioned with a radical photoinitiator, namely 2-hydroxy-2-methyl-1-phenyl propan-1-one and photocrosslinked by UV-curing either as such or while subjected to uniaxial stress. The characteristics of the resulting networks were investigated by means of DSC, XRD, POM, FT-IR, DMTA, and TMA analyses. The effect of UV-curing under stretching and of photoinitiator uptake on the LC phase stability and on the orientation of the networks, as well as on their dynamic-mechanical and thermo-mechanical response are discussed.

© 2009 Elsevier Ltd. All rights reserved.

1. Introduction

Liquid Crystalline Elastomers (LCEs) are lightly cross-linked networks, in which rigid-rod LC molecules are incorporated into the polymer backbone, or linked to it *via* a flexible spacer. In the former case, they are called "main-chain LCE", while in the latter they are known as "side-chain LCE". LCEs typically have low glass transition temperatures, low moduli and exhibit LC phase transitions due to the high mobility of the network strands. Such systems have shown spontaneous shape change at the phase transitions, strain-induced orientational transitions leading to new organized morphologies, peculiar dynamic-mechanical properties and soft elasticity [1–4]. These materials are being studied extensively because of their importance in basic science research as well as for their potential applications in the field of mechanical actuators (artificial muscles), optics and coatings of materials, which can efficiently dissipate mechanical energy for, e.g. automotive and aerospace industry. Their ability to change their shape and size significantly and reversibly at LC to isotropic phase transition, in response to temperature or other external stimuli, has turned one

of their most intriguing features, but parameters such as contraction length, stress and speed of response need to be optimized in order to allow application in robotics, microfluidics and micromechanical systems. For these purposes, LCEs with well-ordered and immobilized mesophases at room temperature are required. First, much investigation was devoted to improve understanding of the physical properties and chemical requirements of side-chain LCEs [5–7]. However, the presence of mesogenic units inserted within the polymeric backbone should induce a stronger coupling between the polymeric chain orientation, network deformation and LC orientational order than side-chain LCEs, as it was confirmed by Wermter and Finkelmann [4]. Several papers have recently appeared, which deal with the synthesis and characterization, as well as elastic and thermoelastic response, of main-chain LCEs obtained by hydrosilylation polyaddition reaction of a bifunctional mesogenic monomer containing two terminal vinyl groups with tetramethyldisiloxane and a pentafunctional crosslinker [8–12]. A new class of main-chain LCEs was obtained by reacting rigid-rod epoxy terminated molecules with aliphatic diacids [13–16]. These materials have been extensively investigated as regards their orientation and mechanical properties [17,18], stress relaxation [18,19] and viscoelasticity [20]. For such materials, a metastable oriented structure was achieved by quenching stretched samples to the glassy state.

* Corresponding author. Tel.: +34 977558174; fax: +34 977559621.
E-mail address: marta.giamberini@urv.net (M. Giamberini).

In this work we explore the possibility of making shape memory main chain LC materials, freezing the induced orientation by means of a photopolymerization process (UV-curing), which involves the allyl functionalities introduced in the mesogenic moieties. For this purpose, we blended a well-known mesogenic diglycidyl-terminated monomer, namely 4,4′-diglycidyloxybiphenyl (DIF), together with different amounts of its homologous bearing lateral photocurable allyl groups (AllDIF). The obtained blends were thermally cured with an aliphatic diacid (decandioic acid, SA), leading to the formation of LC networks in all the cases but 100% AllDIF composition. LC networks corresponding to a selected blend composition (AllDIF/DIF 30/70) were subsequently conditioned with a radical photoinitiator, namely 2-hydroxy-2-methyl-1-phenyl propan-1-one and photocrosslinked by UV-curing either as such or while subjected to uniaxial stress. The characteristics of the resulting networks were investigated by means of Differential Scanning Calorimetry (DSC), X-ray diffraction (XRD), Polarized Optical Microscopy (POM), Fourier-Transform Infra-red spectroscopy (FT-IR), Dynamic-mechanical thermal analysis (DMTA), and Thermo-mechanical Analysis (TMA). The effect of UV-curing under stretching and of photoinitiator uptake on the LC phase stability and on orientation of the networks, as well as on their dynamo-mechanical and thermomechanical response are discussed.

2. Experimental section

2.1. Materials

All reagents were purchased from Aldrich and all the solvents were supplied by Scharlau. They were both used as received without any further purification.

3,3′-diallyl- 4,4′-dihydroxybiphenyl was synthesized as previously reported [21].

3,3′-diallyl-4,4′-diglycidyloxybiphenyl (AllDIF) was synthesized according to the following procedure: 6.8 g (2.54×10^{-2} mol) of 3,3′-diallyl- 4,4′-dihydroxybiphenyl, 15 mL of 2-propanol, 20 mL (0.254 mol) of 1-chloro-2,3-epoxypropane and 4 mL of water were charged into a 100-mL, 3-necked flask equipped with stirrer, condenser, temperature probe and N_2 sweep. While stirring, the mixture was heated to reflux. 2.23 g of NaOH (0.056 mol, 20 wt.-% aqueous solution) was then added dropwise. It was held at reflux for 2 h, then the aqueous layer at the bottom was removed. The organic layer was evaporated in a roto-vap, yielding a yellow oil. The oil was dissolved in 30 mL 4-methyl-2-pentanone and, while heating, 1.02 g of NaOH (5 wt.-% aqueous solution) were added. The solution was held at reflux for 30 min. The aqueous layer was then removed, while the organic layer was evaporated in a roto-vap, yielding a yellow oil which was washed with chloroform and let crystallize on cooling. Finally, it was vacuum filtered and dried. Yield: 32%. ^{13}C NMR ($CDCl_3$, tetramethylsilane (TMS, δ ppm)): 34.7 (Ar-C̲H$_2$–CH=CH$_2$); 44.7 (glycidylic C̲H$_2$); 50.4 (glycidylic C̲H); 69.0 (glycidyl-C̲H$_2$–O); 112.0 (Ar ortho to glycidyloxy and meta to allyl); 115.7 (Ar-CH$_2$–CH=C̲H$_2$); 125.6 (Ar meta to glycidyloxy); 128.6 (Ar para to glycidyloxy); 129.3 (A̲r-CH$_2$–CH=CH$_2$); 134.0 (Ar ortho to allyl and meta to glycidyloxy); 136.9 (Ar-CH$_2$–C̲H=CH$_2$); 155.5 (glycidyloxy-A̲r). ^1H NMR ($CDCl_3$, TMS, δ ppm): 2.8, 2.9 (dd, 2H, glycidylic C̲H$_2$); 3.4 (m, 1H, glycidylic C̲H); 3.5 (d, 2H, Ar-C̲H$_2$–CH=CH$_2$); 4.0, 4.3 (dd, 2H, –O–C̲H$_2$–Gly); 5.1 (dd, 2H, Ar-C̲H$_2$–CH=C̲H$_2$); 6.1 (m, 1H, Ar-CH$_2$–C̲H=CH$_2$); 6.9 (d, 1H, Ar ortho to glycidyl); 7.4 (d, 2H, Ar para and ortho to allyl). Melting point: 52 °C.

4,4′-diglycidyloxybiphenyl (DIF) was synthesized as previously described [22].

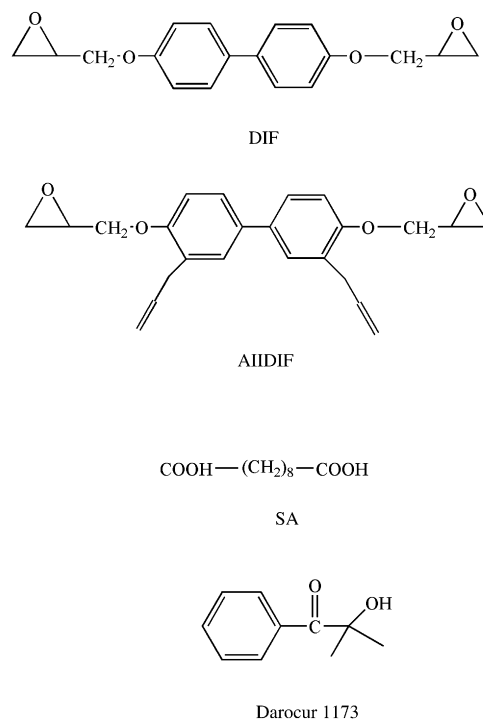The chemical structure of the used compounds is reported in Fig. 1.

Fig. 1. Chemical structure of the used compounds.

Thermally cured samples were prepared from mixtures containing different AllDIF/DIF molar ratios, i.e. 0, 30, 40, 50 and 100%. Resins were cured by mechanically mixing the epoxy compounds, in the selected composition, and decandioic acid (SA, Aldrich, purity $\geq$ 98%), taken in a stoichiometric ratio (1:1 carboxylic group/ glycidylic group). Each mixture was heated to a temperature higher than the melting points of the two components and held at this temperature, under stirring, for 5 min, to make it homogeneous. Successively, it was poured between two glass slides sealed with a silicon gasket, previously treated with a surfactant agent (Surfa-sil®, Pierce), to be thermally cured in oven.

All samples were cured at 180 °C for 90 min. Pressure was cyclically reduced from atmospheric to 150 mmHg in order to allow degassing of samples during the cure.

In the case of the networks obtained from the thermally cured AllDIF/DIF 30%, samples were also subsequently UV-cured by exposing them – 3 not consecutive shots of 10 min exposure – to a UV source (Helios Italquartz vapour pressure Hg lamp, Milano, Italy; intensity on the sample surface: 30 mW/cm^2). For this purpose, some thermally cured AllDIF/DIF 30% samples have been conditioned in 2-hydroxy-2-methyl-1-phenyl propan-1-one (Dar-ocur 1173 from Ciba Specialty Chemicals) as radical photoinitiator for 3 days at r.t.. This time was enough in order to ensure a reasonable diffusion of the liquid photoinitiator into the polymer, for the subsequent UV-curing process. As a matter of fact, we have monitored the photoinitiator uptake for a period of 5 days, in order to find the best compromise between the existence of the LC phase and the uptake of a reasonable amount of photoinitiator suitable for the UV-curing process.

Therefore, some of such conditioned samples were heated at 60 °C, mechanically stressed in order to achieve 150 or 300% of elongation and then subjected to the UV-curing process, in order to freeze the orientation of the mesophases. The physico-mechanical behaviour of such oriented materials was compared to that of unoriented UV-cured samples.

2.2. Characterizations

^{13}C and ^{1}H NMR spectra were recorded at 75.463 and 300.066 MHz, respectively, or 100.626 and 400.145 MHz, on a VARIAN GEMINI (6,1B version with 300 MHz, 6,1C version with 400 MHz), with the applied magnetic field of 7.0 T for 300 MHz and 9.4 T for 400 MHz with proton noise decoupling for [13]C. The spectra were recorded at room temperature with 10–20% (w/v) sample solutions in CDCl$_3$. The central peak of CDCl$_3$ was taken as reference and the chemical shifts are given in ppm from TMS using the appropriate shift conversions.

The photoinitiator uptake (PI$_u$%) was measured by conditioning the samples at room temperature in 2-hydroxy-2-methyl-1-phenyl propan-1-one for different times. The following equation was used:

$$PI_u\% = \frac{w_t - w_0}{w_0} 100$$

where w_0 and w_t are the sample weights at time 0 and time t, respectively.

The residual amount of photoinitiator was removed from the sample after photocuring by treating it with boiling chloroform in a Soxhlet apparatus for 1 h.

Thermal transitions were detected with a Mettler–Toledo differential scanning calorimeter (DSC) mod. 822 in dynamic mode at a heating or cooling rate of 10 °C/min. In isothermal mode, the DSC was stabilized at the temperature of 180 °C, the sample rapidly introduced into the cell, and the experiment started. Nitrogen was used as purge gas. The calorimeter was calibrated with an indium standard (heat flow calibration) and an indium–lead–zinc standard (temperature calibration).

X-ray diffraction patterns were recorded at room temperature by the photographic method using a Rigaku mod. III/D max generator, or with a Siemens D5000 diffractometer in the θ–θ configuration, fitted with an Anton Paar TTK temperature chamber. CuK$_\alpha$ radiation was used and graphite was the second monochromator. The Bragg angle step was 0.05° and the time per step 3 s. Pole figures were recorded at room temperature on a Siemens D5000 diffractometer equipped with a goniometer that had an open Eulerian cradle; CuK$_\alpha$ radiation was used.

The degree of orientation of the stretched networks was estimated from XRD patterns according to Chistyakov and Chaikowsky [23].

FT-IR spectroscopy was used to follow the curing process and to assure the stability of the allyl group during the thermal curing. FT-IR analyses were performed by using a 680PLUS Jasco spectrometer in the absorbance mode, coupled with an ATR (Attenuated Total Reflection mode) Golden Gate Specac-Teknokroma with a temperature control; the sample was put onto a diamond crystal. The spectra were collected using 32 scans at 4 cm^{-1} resolution, in the 400–4000 cm^{-1} region.

In order to check the effectiveness of the photopolymerization reaction, FT-IR–ATR spectra were collected by using a Nicolet 5700 apparatus, equipped with a Small Orbit accessory and a diamond crystal. The ATR spectra were collected using 256 scans at 4 cm^{-1} resolution, in the 600–4000 cm^{-1} region.

Textures of the samples were observed by means of an Axiolab Zeiss optical microscope equipped with a Linkam TP92 hot stage.

Dynamic-mechanical analyses (DMTA) were performed on a MK III Rheometrics Scientific Instr. at 1 Hz frequency in the tensile configuration. Moreover, multi-frequency experiments (ranging from 0.1 to 30 Hz) were performed. The size of the specimen was about $8 \times 4 \times 0.5$ mm. The storage modulus, E', and the loss factor, tan δ, were measured from r.t. up to the temperature at which all the first and second order transitions were attained. The Tg value was assumed as the maximum of the loss factor curve vs. T.

Thermomechanical (TMA) experiments were performed by employing a Mettler TMA 40 Instr. in the tensile configuration (static force: 0.020 N): the samples were heated up to 120 °C at 5 °C/min, then cooled down to r.t. (cooling rate: −5 °C/min).

3. Results and discussion

3.1. Preparation of LCEs

The reaction between epoxy and carboxylic groups in the molten state is well-known and has been widely used to prepare cross-linked casting and laminates, as well as elastomeric systems [24]. The epoxy-acid chemistry is complex since it involves different possible reactions: the most important reactions which take place in the stoichiometric formulations are the epoxy-acid addition, the transesterification of the resulting β-hydroxyester, as well as the condensation between the acid and the hydroxyl group [25–27]. The alkoxide anions generated by the epoxy ring opening catalyze transesterification and also initiate the epoxy homopolymerization [28,29]. The occurrence of these side-reactions allows to obtain a lightly cross-linked material also in the case of 1:1 epoxy/carboxyl stoichiometry, when the reaction is performed in the molten state.

In order to find the best compromise between ordered structure in the thermally cured network and possibility to orient the material by stretching it in the rubbery state and subsequently enhance its crosslink density by UV-curing, we investigated the behaviour of mixtures AllDIF/DIF containing different amounts of AllDIF, thermally cured with decandioic acid. Although DIF is not a liquid crystalline compound itself, it was found able to generate mesomorphic structures upon curing with amines [22,30], anhydrides [24] as well as carboxylic acids [14]. AllDIF was obtained by glycidyl termination of 3,3′-diallyl- 4,4′-dihydroxybiphenyl and it is not a mesogenic compound, clearly due to the presence of the lateral allyl groups which perturb the interactions among the rigid moieties.

Fig. 2 shows the FT-IR spectra between 2000 and 700 cm^{-1} of a mixture of AllDIF/DIF (30 mol.%) and stoichiometric amount of decandioic acid after 1 min (a) and 90 min (b) of thermal cure at 180 °C. From the comparison of the spectra, it can be noticed that the peak at 1710 cm^{-1}, which was ascribed to the stretching of the acid carbonyl group, is shifted to 1734 cm^{-1} after 90 min of reaction, thus confirming the conversion of the acid to ester group. No variations could be observed in the small peak at 1636 cm^{-1} nor in
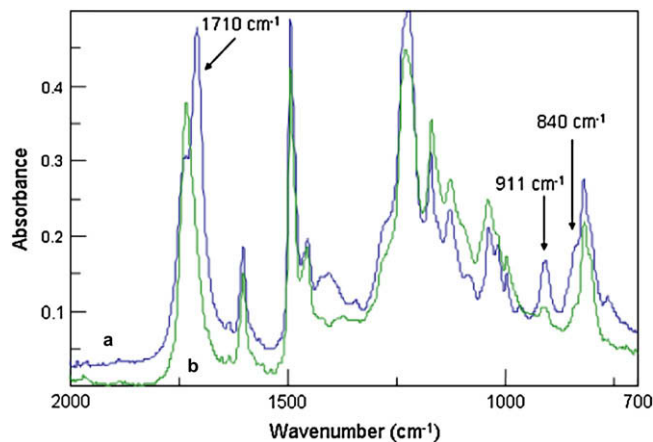

Fig. 2. FTIR spectra between 2000 and 700 cm^{-1} of a mixture of AllDIF/DIF (30 mol.%) and stoichiometric amount of SA after 1 min (a) and 90 min (b) of thermal cure at 180 °C.

Table 1
Characteristics of the materials with different AllDIF/DIF ratios, obtained by thermal curing with SA at 180 °C.

System (% AllDIF)	Tg (°C)[a]	Tc (°C)[a]	Clearing enthalpy[b] (kJ/mol)	Clearing entropy[b] (J/mol K)	d (Å)
0	56	139	21.1	51.2	14.5
30	45	101	8.5	22.7	14.4
40	30	67	4.5	13.2	14.7
50	21	55	3.6	11.0	15.0
100	0	n.e.	n.e.	n.e.	n.e.

n.e.: not evident.
[a] From DSC second heating scan.
[b] Normalized with respect to the moles of epoxy and acid units.

the peak at 1000 cm^{-1}, which were attributed to C=C stretching and =C–H bending of the allyl group, respectively. In the spectrum recorded after 1 min cure, a quite broad peak was observed at about 911 cm^{-1}, which included both epoxy ring deformation and out-of-plane vibration of C=C–H groups; the intensity of this peak decreased noticeably after 90 min reaction. Moreover, a considerable decrease of the peak at 840 cm^{-1}, which was attributed to epoxy ring vibration, was evident after 90 min reaction. These evidences suggested that thermal curing occurred through reaction of epoxy and carboxylic groups, while the allyl groups were not affected by the thermal treatment at 180 °C during 90 min. After this thermal curing, the AllDIF/DIF-SA mixtures gave rise to materials almost completely insoluble in several solvents of different polarities with glass transition temperatures (Tg) lying between 0 and 56 °C. Table 1 reports the characteristics of the materials with different AllDIF/DIF ratios, obtained by thermal curing. In all cases but 100% AllDIF/DIF sample, networks with a smectic structure were obtained. On increasing the amount of AllDIF, a decrease of Tg was observed, as expected due to the presence of lateral allyl groups: in general, flexible pendant groups reduce the Tg of the polymer by lowering the frictional interactions between chains and thus reducing the rotational energy requirements of the backbone. Lower Tg values could also be attributable to lower cross-linking degrees. We could not get exhaustive information about the extent of curing of the different mixtures from curing enthalpies as measured by isothermal DSC experiments at 180 °C: these data ranged between about 100 and 150 kJ/mol and were very scattered, reasonably due to the experimental error related to the sample introduction in DSC cell at the desired temperature. For this reason, we could not exclude that the presence of allyl groups also affected

the reaction extent between epoxy groups and carboxylic acid, reasonably due to steric hindrance.

The clearing temperature of the networks also showed a decreasing trend on increasing the amount of AllDIF: this is in agreement with non-LC nature of this compound, which acted as a "diluent", thus perturbing the ordered structure of the thermoset. The trend of the clearing enthalpy and entropy was also coherent with this hypothesis, as they both decreased on increasing the amount of AllDIF. The smectic layer thickness was slightly affected by the amount of allyl compound and was in the range 14.5–15 Å.

3.2. Orientation of LCEs

We explored the possibility to orient the thermally cured samples by stretching, and subsequently stabilize the achieved orientation by increasing the cross-linking density. In previous papers [13,15,18], some different attempts were performed in order to freeze the achieved orientation by simply quenching samples below their Tg value. Such procedure was limited by the fact that in this case the frozen metastable orientation could be simply lost by heating the samples above their Tg. Therefore, we tried to induce the formation of a stable oriented network by increasing the cross-linking density of the stretched materials through photo-polymerization of the lateral allyl groups. First, we dissolved a solid photoinitiator, namely 2,2-dimethoxy-2-phenyl acetophenone (Irgacure 651), in chloroform (0.2 wt.%) and let the elastomeric sample swell in this solution for 45 min; then, the sample was vacuum dried at room temperature. Fig. 3a shows the X-ray diffraction pattern of AllDIF/DIF 50% mixture cured with SA for 90 min at 180 °C, treated with the photoinitiator as previously described, and stretched at 60 °C to relative elongation $\Delta l/l_0 = 0.9$ (with $\Delta l = l_{stretched} - l_0$). A diffraction corresponding to $d = 15.0$ Å, typical of an oriented smectic mesophase, was evident in the equatorial plane, while no orientation was exhibited by the lateral distance between mesogens at $d = 4.0$ Å (diffuse halo). The slight orientation in this case seemed to be dominated by the smectic layers, as they orient parallel to the stretching direction. The XRD pattern of the same sample previously soaked in the photoinitiator solution and subsequently exposed to a very low-power UV source (1 mW/cm^2) for 30 min is showed in Fig. 3b. In this case, the diffraction at $d = 15.0$ Å was found in the meridional plane, which means that the smectic layers oriented perpendicular to the stretching direction, i.e. the orientation was dominated by the polymer chains. This is in agreement with an increase in
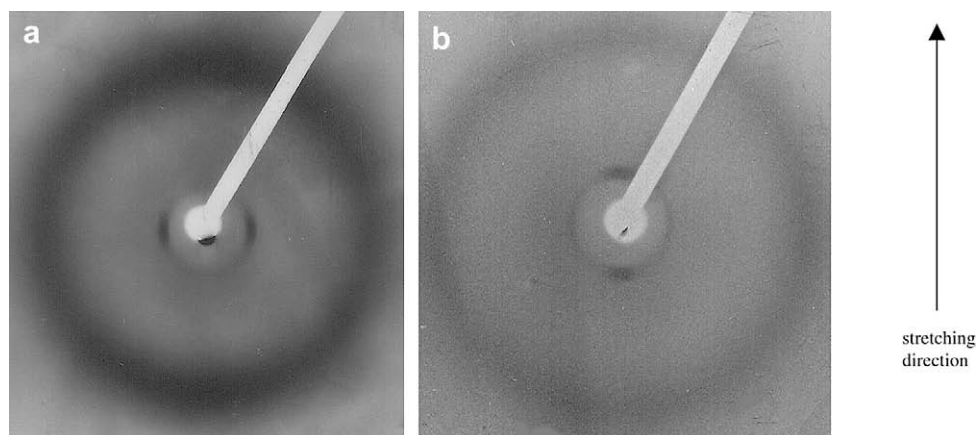

↑
stretching direction

Fig. 3. X-ray diffraction pattern of AllDIF/DIF 50% mixture cured with SA for 90 min at 180 °C, swollen in chloroform solution of 2,2-dimethoxy-2-phenyl acetophenon (0.2 wt.%), vacuum dried at room temperature and stretched at 60 °C to relative elongation $\Delta l/l_0 = 0.9$ before (a) and after (b) exposure to UV source (1 mW/cm^2) for 30 min.

cross-linking density as a consequence of UV irradiation [31,32]. However, a limited increase of cross-linking density could be obtained in this case, as inferred from FT-IR and DSC experiments, reasonably due to both the poor interaction between the photo-initiator and the elastomer, and the low power of the UV source. Therefore, we decided to select a liquid photoinitiator, 2-hydroxy-2-methyl-1-phenyl propan-1-one, and to use a higher power UV lamp.

In order to perform a deeper investigation, among the different mixtures we selected the sample containing 30% AllDIF as it had a relatively low Tg value (32 °C), which should make it quite easily oriented by stretching at relatively low temperatures, and at the same time exhibited a quite high clearing temperature (78.5 °C).

Fig. 4 reports the FT-IR spectra of AllDIF/DIF 30% mixture cured with SA for 90 min at 180 °C before (a) and after UV irradiation (3 not consecutive shots of 10 min) (b). The differences between the two spectra mainly were in the disappearance of the peak at 914 cm^{-1} and in the decrease of the intensity of the peak at 808 cm^{-1}. Both these peaks could be attributed to the out-of-plane deformation of the allyl groups; thus their change indicated that UV-curing reaction took place. In the UV-cured sample, the appearance of a band at 1674 cm^{-1} is evident. From a comparison with the FT-IR spectrum of the neat photoinitiator, this band could be attributed to the carbonyl group stretching of the photoinitiator itself, thus indicating that a noticeable amount is still present in the final network.

As previously mentioned, we monitored the photoinitiator uptake for a period of 5 days and investigated its effect on the stability of the LC phase and on Tg, since it can act as plasticizer, lowering the glass transition temperature of the network. Although this, in turn, may facilitate the network orientation, it could also adversely affect the interactions between mesogens, which are responsible for the LC structure. The data collected in Table 2 indicate that the photoinitiator uptake, even if it is quite high, starts to have a significant effect on the LC phase only after three days of conditioning. Afterwards, no LC phase could be found in the samples conditioned for 4 days; in this case, a significant decrease of the Tg values can be observed, thus confirming the plasticizing effect of the photoinitiator. For all these reasons, we decided to photopolymerize and to investigate all the AllDIF/DIF samples after conditioning for three days in the liquid photoinitiator. The presence of photoinitiator also in the UV-cured samples was evidenced through DMTA experiments as discussed later.
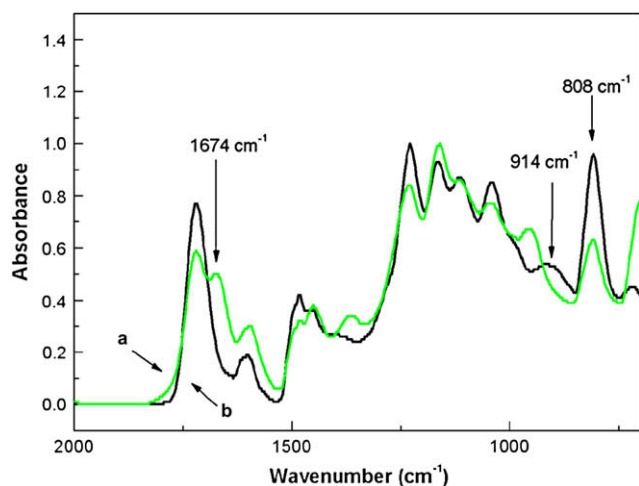
3.3. DMTA, DSC and XRD characterization of the AllDIF/DIF 30% LCEs

Fig. 5 reports the typical DMTA spectrum of the AllDIF/DIF 30% mixture after thermal curing with SA: the tan δ peak located at 79.6 °C can be attributed to the clearing of the sample; the Tg of the LC elastomer is hidden by the clearing peak. In order to demonstrate this, multi-frequency DMTA runs were performed: the maximum of tan δ peak was very slightly influenced by the applied frequency, thus indicating that the peak is not attributable to a second-order transition. Furthermore, as reported in Fig. 6, after having conditioned the AllDIF/DIF 30% sample for three days in the photoinitiator, the tan δ peak of the starting material splits into two peaks: the former has a high intensity and is located at higher temperatures (89.5 °C) and can be referred to the clearing of the material; the latter has a weaker signal and corresponds to lower temperatures (42 °C) and can be attributed to the glass transition temperature of the amorphous domains, in the presence of unreacted photoinitiator, which acts as a plasticizer.

Table 3 reports the characteristics (DSC and XRD data) of the elastomers obtained from the AllDIF/DIF 30% mixture after thermal curing, before and after exposure to UV irradiation.

As it can be seen, the sample obtained after conditioning in the photoinitiator and subsequent photocuring (UV – Table 3) still exhibits a smectic structure with a distance between layers equal to 14.4 Å, the same as in the case of the sample before exposure to UV light (TC – Table 3). After the Tg step, in all cases an endothermic peak was observed in DSC heating scans, which corresponds to the clearing point of the samples, as confirmed by XRD analyses performed at 130 °C. A slight decrease in the clearing temperature, which changed from about 100 to 92 °C, is observed: it can be attributable to the presence of residual photoinitiator, which, also in this case, acts as a plasticizer. Moreover, the additional crosslinks formed by the lateral allyl groups in the photocured sample reasonably increase the amorphous fraction in the sample, thus determining lower clearing enthalpy and entropy values.

As far as DMTA is concerned, Fig. 7 shows the DMTA spectrum of the sample conditioned in the photoinitiator (for three days) and then UV-cured. Tan δ curve evidences the presence of two partially overlapped peaks: the former is located at 46.7 °C and can be related to the Tg of the material, the latter at 79.6 °C can be attributed to the clearing phenomenon. Moreover, a further increase of the conditioning time of the sample in the photoinitiator leads to the complete disappearance of the tan δ peak related to the clearing point: in this case, the tan δ peak, located at lower temperatures (i.e. about 20 °C), could be detected and attributed, according to DSC data, to the Tg.

In order to achieve orientation of the mesophase and subsequently freeze it, samples of AllDIF/DIF 30% mixture after thermal curing with SA were conditioned in the photoinitiator for three days, heated at 60 °C, mechanically stressed in order to achieve 150

Fig. 4. FTIR spectra of AllDIF/DIF 30% mixture cured with SA for 90 min at 180 °C before (a) and after UV irradiation (3 not consecutive shots of 10 min) (b).

Table 2
Effect of the photoinitiator (PI) uptake on thermal and LC properties of AllDIF/DIF 30% mixture cured with SA.

Time in PI (days)	PI uptake (wt.%)	Tg (°C)[a]	Tc (°C)[b]	Clearing enthalpy (kJ/mol)[b]
0	0	45	101	8.5
1	5.7	44	100	7.4
2	11.6	45	102	7.6
3	22.4	46	101	6.2
4	40.4	37	n.e.	n.e.

n.e.: not evident.
[a] Glass transition temperature from DSC first heating scan.
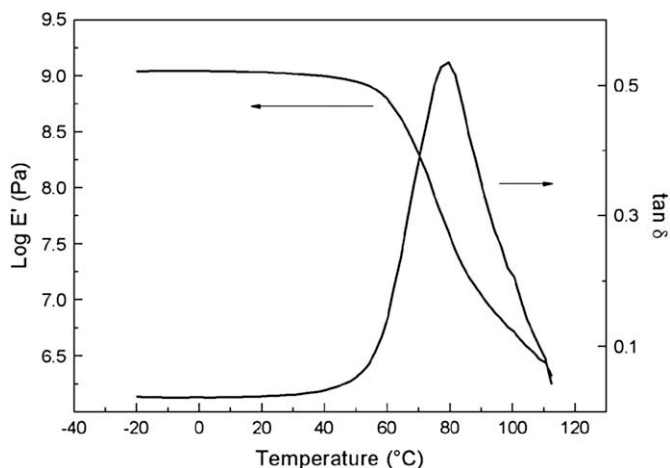[b] Clearing temperature and enthalpy, respectively, from DSC first heating scan.

Fig. 5. DMTA spectrum of the AllDIF/DIF 30% mixture after thermal curing with SA.

System	Tg (°C)	Tc (°C)	Clearing enthalpy (kJ/mol)	Clearing entropy (J/mol K)	Mesophase	Spacing (Å)
TC[a]	45	101	8.5	22.7	Smectic	14.4
UV[b]	46	92	7.0	19.2	Smectic	14.4
ST[c]	40	96	6.7	18.2	Nematic	–
ST2[d]	53	103	4.9	13.0	Nematic	–

[a] Thermally cured.
[b] Thermally cured, then UV cured.
[c] Thermally cured, stretched (300%) and UV cured.
[d] Sample ST after treatment with boiling chloroform.

enthalpy and entropy and a modest increase of Tc [33]. This behaviour is confirmed by DMTA analyses (Fig. 9), which show a low Tg halo together with a peak attributed to the clearing point (79 °C).

3.4. Evaluation of the elastic response of stretched UV-cured LCEs

In order to check the elastic response of the aforementioned stretched UV-cured samples, thermomechanical analyses (TMA) were performed and compared to the behaviour of the sample subjected only to thermal curing.

Fig. 10 shows a thermoelastic experiment performed on both heating and cooling cycles at 5 °C/min on AllDIF/DIF 30% mixture after thermal curing with SA, stretched up to 300% relative elongation in the rubbery state and then quenched to the glassy state in order to retain the achieved orientation. In these experiments, the strain was measured as a function of temperature at constant applied load (0.020 N, corresponding to 10 kPa) over a temperature range covering the smectic to isotropic phase transition. The length of the sample remained constant at the lowest temperatures measured in the LC phase and started to decrease at about 70 °C, as the isotropic phase was approached. At the LC-to-isotropic phase transition a sharp decrease in length was observed, whose extent depended on the applied constant stress, as we checked by performing experiments under different values of the applied stress (from 6 to 328 kPa). On cooling, after a hysteresis of about 20 °C, although the process was reversed with a sharp increase in length on going from the isotropic to the LC phase, the dimensional recovery was only 15% and the orientation of the sample was completely lost, as confirmed by XRD. The lower the applied stress, the higher the film contraction on heating through the clearing

or 300% of elongation respectively and then subjected to the UV-curing process while kept stretched. The resulting samples were completely transparent and still exhibited a mesogenic structure, as shown by POM. However, XRD analyses put into evidence only a halo at 2ϑ about 21.3°, which correspond to a spacing of about 4.2 Å; the photocured stretched sample thus exhibited nematic structure. For both 150% and 300% stretched UV-cured samples, the pole figures corresponding to the halo at $2\vartheta = 21.3°$ show a good degree of orientation of the mesogen in the stretching direction (e.g. Fig. 8 shows XRD 300% stretched UV-cured sample): from azimuthal scans performed on their XRD patterns, values of the order parameter 0.5 and 0.6, for 150 and 300% elongation respectively, were estimated.

The presence of the less ordered nematic phase in the case of the stretched and subsequently photocured samples could be explained as follows: first, the mechanical stress forces the mesogens to align along the stretching direction. Subsequently, cross-links increase as a consequence of photocuring, and act as constraints which prevent the stretched network from arranging in an ordered layered structure.

XRD data can be also related to the DSC results collected in Table 3 for the 300% stretched UV-cured sample: the change from unoriented smectic (UV sample, Table 3) to oriented nematic phase (ST sample, Table 3) determines a slight decrease of the clearing
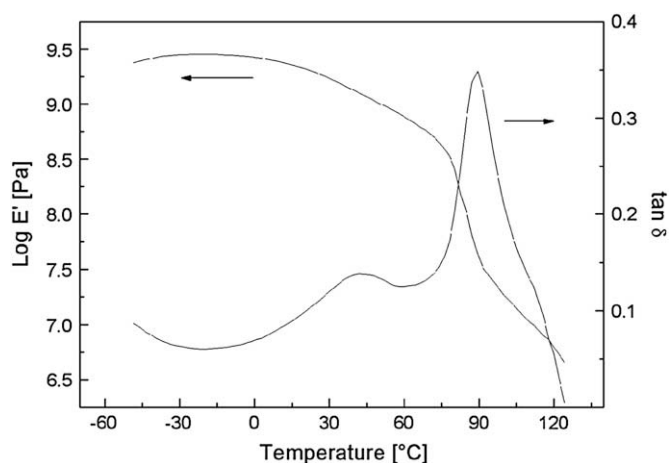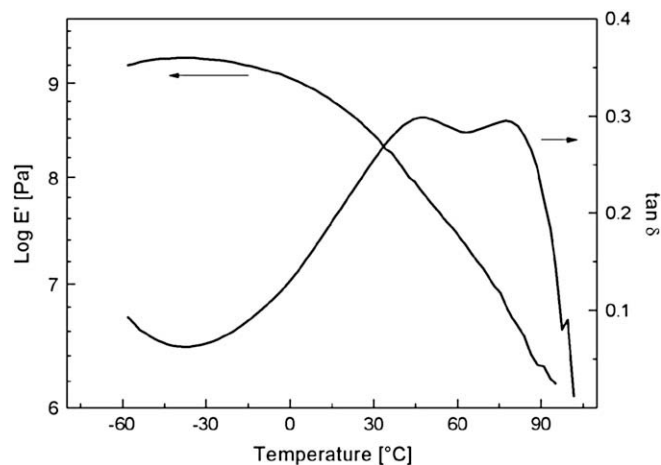

Fig. 6. DMTA spectrum of the AllDIF/DIF 30% mixture after thermal curing with SA and conditioning in the photoinitiator (2-hydroxy-2-methyl-1-phenyl propan-1-one) for three days.

Fig. 7. DMTA spectrum of the AllDIF/DIF 30% mixture thermally cured with SA, conditioned in the photoinitiator for three days and then UV-cured.
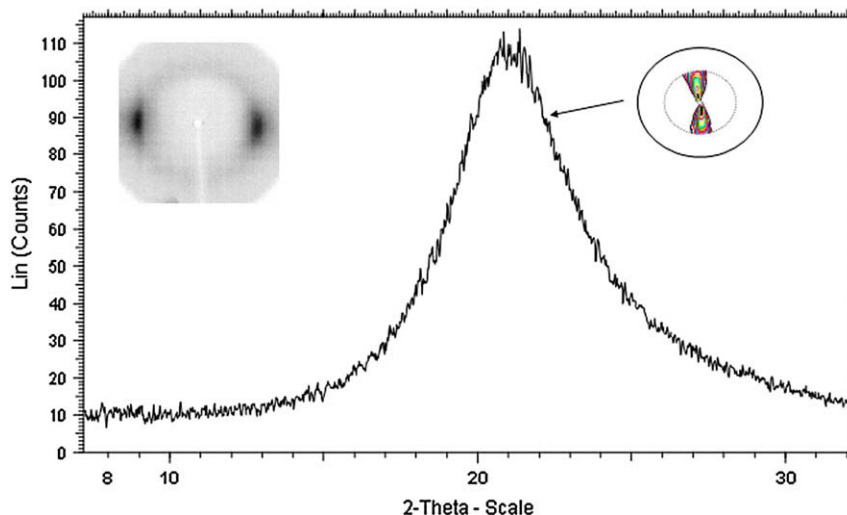
Fig. 8. Wide-angle X-ray diffractogram of AllDIF/DIF 30% mixture thermally cured with SA, conditioned in the photoinitiator for three days and then UV-cured while subjected to 300% elongation; in the insets the corresponding pole figure (right side) and the photographic pattern image (left side) are shown.

point and the lower the elongation in the cooling step: in other words, dimensional recovery was more efficient in the case of higher values of the applied stress. Obviously, in such conditions, the applied tensional stress tended to oppose to film contraction, while it favoured film elongation. In any case, on increasing the applied stress from 6.2 to 328 kPa, film contractions ranging between 46 and 13% were observed, with subsequent dimensional recoveries in between 15 and 12%, respectively. Therefore, the system after thermal curing was unable to retain the orientation achieved upon stretching and exhibited a relatively efficient shape memory effect only at high stresses.

Thermoelastic experiments performed on 150% and 300% stretched UV-cured samples are reported in Figs. 11 and 12. In these experiments, the samples were subjected to 22.5 kPa and 30.8 kPa stress, respectively. At the nematic to isotropic phase transition, a sharp decrease in length of about 3.5% was observed. On cooling, the process was completely reversed with a sharp increase in length on going from the isotropic to nematic phase. A small hysteresis in temperature was observed, which could be due to a small temperature lag between the sample and the thermocouple. XRD analyses performed on the samples after TMA

experiments showed that they completely recovered their orientation after heating/cooling cycles.

The poor dimensional variation we encountered in the TMA experiments reported in Figs. 11 and 12 can be substantially attributed to the higher degree of cross-linking in the material, due to the additional UV treatment. In order to verify this hypothesis, we treated the sample ST, obtained after thermal curing, 300% stretching and UV-curing, with boiling chloroform in order to remove the residual photoinitiator, and we finally vacuum dried the sample. Unfortunately, the sample did not tolerate the treatment with the boiling solvent: many cracks appeared and fragmentation occurred, which prevented us from repeating TMA experiments on this sample. However, we performed DSC analysis (the same ramp-up/cooling down/ramp-up cycle we used for the thermal characterization of the elastomers) on such fragmented sample. We found (Table 3, sample ST2) that the residual photoinitiator removal determined an increase of the sample T_g (from 40 to 53 °C), a slight increase of T_c (from 96 up to 103 °C) and a decrease of both clearing enthalpy (from 6.7 to 4.9 kJ/mol) and entropy (from 18.2 to 13 J/(mol K)). However, we cannot exclude that the presence of considerable amount of residual photoinitiator may also limit the
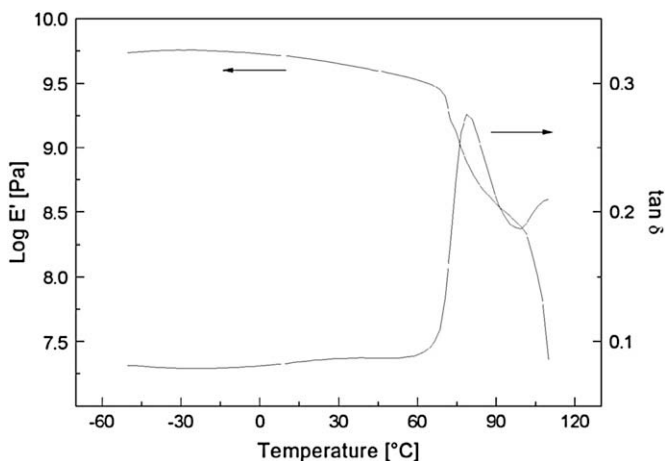

Fig. 9. DMTA spectrum of AllDIF/DIF 30% mixture thermally cured with SA, conditioned in the photoinitiator for three days and then UV-cured while subjected to 300% elongation.
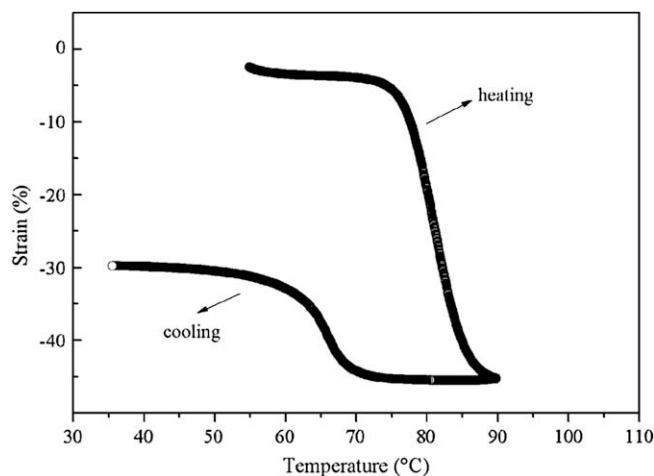

Fig. 10. TMA experiment performed on both heating and cooling cycles at 5 °C/min on AllDIF/DIF 30% mixture after thermal curing with SA, stretched up to 300% relative elongation in the rubbery state and then quenched to the glassy state.
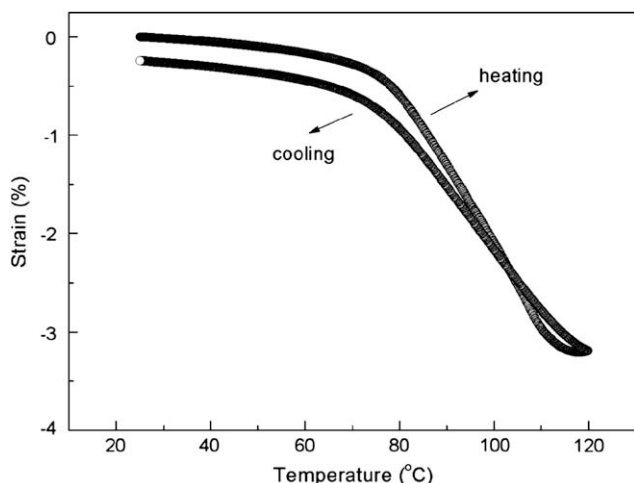
Fig. 11. TMA experiment performed, on both heating and cooling cycles at 5 °C/min, on AllDIF/DIF 30% mixture thermally cured with SA and subsequently UV-cured while subjected to 150% elongation.

extent of LC domains, since we found that by conditioning the LC elastomers in the liquid photoinitiator, a considerable decrease of the clearing enthalpy was put into evidence, as previously described.

The approach we describe represents a first attempt in order to get novel main chain LC materials, which exhibit shape memory properties. Although we were successful in freezing the induced orientation, higher dimensional variations should be obtained in order to be able to potentially use such materials as actuators. For this purpose, blends with different compositions should be investigated in order to reach a better compromise between the amount of allyl groups in the blend, which are necessary in order to freeze the orientation of the LC phase in the stretched sample, and the dimensional variation at the phase transition, which needs to be higher for the material to work as actuator.

4. Conclusions

In this paper, we examined the behaviour of blends of a well-known mesogenic diglycidyl-terminated monomer, namely
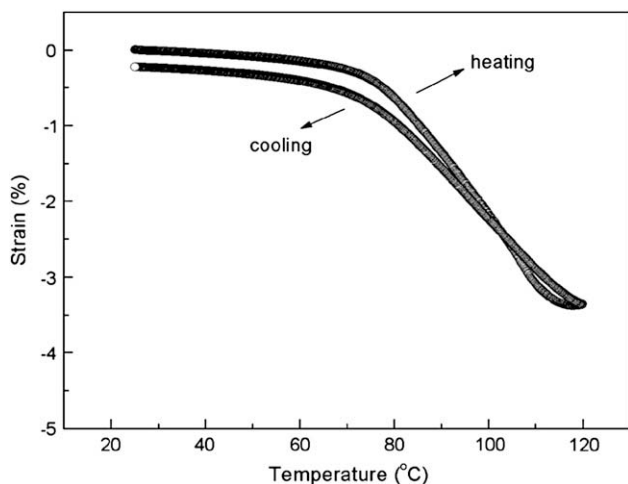

Fig. 12. TMA experiment performed, on both heating and cooling cycles at 5 °C/min, on AllDIF/DIF 30% mixture thermally cured with SA and subsequently UV-cured while subjected to 300% elongation.

4,4′-diglycidyloxybiphenyl (DIF), together with different amounts of its homologous bearing lateral photocurable allyl groups (All-DIF), after a dual-curing process, first thermal- and subsequently UV-activated. By this strategy, we tried to prepare shape memory main chain LC elastomers. First, blends were thermally cured with stoichiometric amounts of decandioic acid and gave rise to smectic elastomers in all the investigated compositions except for 100% AllDIF. In general, according to the trends of clearing temperatures, enthalpies and entropies, the presence of this monomer seems to perturb the ordered structure of the network. Subsequently, a selected blend with 30 mol% AllDIF was conditioned with a radical liquid photoinitiator for three days and photo-polymerized both as such and while subjected to uniaxial stress. The conditioning time was selected on the basis of photoinitiator uptake, which is quite high and starts to have a significant effect on the LC phase after three days of conditioning. LC elastomers were obtained in both cases, namely polydomain smectic in the former case and oriented nematic in the latter, as revealed by XRD, DSC and POM.

The resulting networks were also characterized by means of DMTA analysis. The presence of residual photoinitiator was shown to have noticeable consequences on the extent of LC domains.

As far as thermomechanical response is concerned, we compared the behaviour of the AllDIF/DIF 30% mixture after thermal curing with SA, stretched in the rubbery state and then quenched to the glassy state, in order to retain the achieved orientation, with the behaviour of elastomers obtained after subsequent UV-photocuring while in the oriented state. In the former case, the material was unable to retain the orientation achieved upon stretching and exhibited a relatively efficient shape memory effect only at high values of the applied stress; differently, the elastomers also subjected to UV-curing in the oriented state completely recovered their orientation after heating/cooling cycles. However, only a poor dimensional variation could be obtained in this case: this was ascribed to the higher degree of cross-linking in the material; in any case a reduction of the extent of LC domains in the final network due to the presence of residual photoinitiator could not be ruled out.

References

[1] Warner M, Terentjev EM. Prog Polym Sci 1996;21:853–91.
[2] Stannarius R, Köhler R, Dietrich U, Tolksdorf C, Zentel R. Phys Rev E 2002; 65:41707.
[3] Thomsen III DL, Keller P, Naciri J, Pink R, Jeon H, Shenoy D, et al. Macromolecules 2001;34:5868–75.
[4] Wermter H, Finkelmann H. E-Polymers 2001:013.
[5] Brand HR, Finkelmann H. Physical properties of liquid crystalline elastomers. In: Demus D, Goodby J, Gray J, Spiess HW, Vill V, editors. Handbook of liquid crystals. Weinheim: Wiley-VCH; 1998. p. 277.
[6] Clarke SM, Terentjev EM, Kundler I, Finkelmann H. Macromolecules 1998; 31:4862–72.
[7] Warner M, Terentjev EM. Liquid crystal elastomers. Oxford University Press; 2003.
[8] Donnio B, Wermter H, Finkelmann H. Macromolecules 2000;33:7724–9.
[9] Rousseau IA, Mather PT. J Am Chem Soc 2003;125:15300–1.
[10] Sánchez-Ferrer A, Finkelmann H. Macromolecules 2008;41:970–80.
[11] Bispo M, Guillon D, Donnio B, Finkelmann H. Macromolecules 2008;41:3098–108.
[12] Burke KA, Mather PT. Polym Prepr (Am Chem Soc Polym Chem Div) 2008;49:1091–2.
[13] Giamberini M, Amendola E, Carfagna C. Macromol Rapid Commun 1995;16:97–105.
[14] Giamberini M, Amendola E, Carfagna C. Macromol Chem Phys 1997;198: 3185–96.
[15] Ambrogi V, Giamberini M, Cerruti P, Pucci P, Menna N, Mascolo R, et al. Polymer 2005;46:2105–21.
[16] Ribera D, Giamberini M, Serra A, Mantecón A. J Polym Sci Part A Polym Chem 2006;44:6270–86.
[17] Ortiz C, Wagner M, Bhargava N, Ober CK, Kramer EJ. Macromolecules 1998;31:8531–9.
[18] Giamberini M, Cerruti P, Ambrogi V, Vestito C, Covino F, Carfagna C. Polymer 2005;46:9113–25.

[19] Ortiz C, Ober CK, Kramer EJ. Polymer 1998;39:3713–8.
[20] Giamberini M, Ambrogi V, Cerruti P, Carfagna C. Polymer 2006;47:4490–6.
[21] Caruso U, Iannelli P, Roviello A, Sirigu A. J Polym Sci Part B Polym Phys 1998;36:2371–8.
[22] Giamberini M, Amendola E, Carfagna C. Mol Cryst Liq Cryst 1995;266:9–22.
[23] Chistyakov IG, Chaikowsky WM. Mol Cryst Liq Cryst 1969;7:269–77.
[24] Punchaipetch P, Ambrogi V, Giamberini M, Brostow W, Carfagna C, D'Souza NA. Polymer 2001;42:2067.
[25] Matěka L, Pokorny S, Dušek K. Polym Bull (Berlin) 1982;7:123.
[26] Dušek K, Matěka L. Adv Chem Ser 1984;208:15.
[27] Tanaka Y, Bauer RS. In: May CA, editor. Epoxy resins chemistry and technology. 2nd ed. New York: Marcel Dekker; 1988. p. 285–463.
[28] Craun JP. J Coat Technol 1995;67:841.
[29] Craun JP, Kuo Y, Neag CM. Prog Org Coat 1996;29:55.
[30] Carfagna C, Amendola E, Giamberini M, Filippov AG, Bauer RS. Liq Cryst 1993;13:571.
[31] Canessa G, Reck B, Reckert G, Zentel R. Makromol Chem Macromol Symp 1986;4:91–101.
[32] Krigbaum WR, Watanabe J. Polymer 1983;24:1299.
[33] de Gennes PG. In: Ciferri A, Krigbaum WR, Meyer RB, editors. Polymer liquid crystals. New York: Academic Press; 1982.